Physics of Fluids

Microscopic characterization of fatty liver-based emulsions: Bridging microstructure and texture in foie gras and pâté

Cite as: Phys. Fluids **33**, 117119 (2021); https://doi.org/10.1063/5.0070998
Submitted: 10 September 2021 • Accepted: 18 October 2021 • Published Online: 30 November 2021

Matias A. Via, Mathias Baechle, Alexander Stephan, et al.

COLLECTIONS

Paper published as part of the special topic on Kitchen Flows

This paper was selected as Featured

Physics of Fluids ARTICLE scitation.org/journal/phf

Microscopic characterization of fatty liver-based emulsions: Bridging microstructure and texture in foie gras and pâté

Cite as: Phys. Fluids **33**, 117119 (2021); doi: 10.1063/5.0070998
Submitted: 10 September 2021 · Accepted: 18 October 2021 ·
Published Online: 30 November 2021

Matias A. Via,[1] Mathias Baechle,[2] Alexander Stephan,[3] Thomas A. Vilgis,[2,a)] and Mathias P. Clausen[1,a)]

AFFILIATIONS

[1]Department of Green Technology, University of Southern Denmark, Odense, Denmark
[2]Max Planck Institute for Polymer Research, Mainz, Germany
[3]VAN HEES GmbH, Kurt-van-Hees-Straße 1, 65396 Walluf, Germany

Note: This paper is part of the special topic, Kitchen Flows.
[a)]**Authors to whom correspondence should be addressed:** vilgis@mpip-mainz.mpg.de and mpc@igt.sdu.dk

ABSTRACT

An analysis of food materials often involves characterization of the molecular composition of the food matrix and measuring its mechanical properties. However, there is a gap in understanding how food materials organize at the microscopic level. This article shows the application of minimally invasive coherent anti-Stokes Raman scattering (CARS) microscopy to visualize the fat distribution in duck liver-based products. Further, in combination with quantitative image analysis, CARS provides a viable route for understanding how food texture is related to food microstructure. Strong correlations were found between microscopic structural descriptors of the fat particle (abundance, shape, and size) and rheological and textural parameters (hardness, storage modulus). Foie gras was found to have an irregular shaped fat network connected via relatively weak links that yield under stress correlating with foie gras being harder, more elastic, and more brittle in comparison with a homemade duck liver pâté. In turn, the higher total number of fat particles, more round and smooth in shape, found in the pâté was responsible for it being softer and less prone to fracture. Understanding the relation between molecular composition, microscopic structure, and macroscopic texture provides opportunities for future modification of pâté formulation and/or a new preparation technique using microstructure as a texture indicator.

I. INTRODUCTION

Correct texture of food has a crucial influence on the enjoyment of eating and acceptance of new food.[1,2] Texture is often studied recording the mechanical properties of food materials and relating these to the composition and physicochemical state of the food or by sensory evaluation. However, the underlying microscopic structures and rearrangements that, to a large extent, determine food appearance, texture, and handling properties remain more elusive. Insight into such microstructures therefore provides a valuable route for gaining a more complete gastrophysical (physics of gastronomy)[3] understanding of the relation between structure and function, and sensory properties of food materials. This, in turn, allows us to bridge information from the molecular to the macroscopic scale and provides opportunities for better control and optimization of food preparation and processing.

Foie gras (*literal meaning: fatty liver*) is considered a delicacy and is highly appreciated for its unique textural properties. It is a food product based on the fatty liver of duck or goose typically produced as a sliceable whole liver organ (*entier*)[4] or as a mechanically reconstituted block of different homogenized pieces of foie gras (*bloc*).[5] From a soft matter point of view, foie gras *bloc* is, in analogy to comminuted meat products, a multiphasic system comprised of a continuous phase consisting of proteins, salts, water, carbohydrates, and fibrous particles, and a dispersed phase consisting of solid fat particles, liquid fat globules, and non-soluble meat components.[6] Technically, it can be described as composite material that contains fat particles emulsified in a protein gel matrix, but the term meat batter or meat emulsion is also often used.[7,8]

Production of foie gras exploits the natural tendency of these migratory birds to accumulate fat in the liver and often involves

force-feeding.[4] Liver products from force-fed sources score considerably higher in sensory evaluation in texture, taste, and smell attributes as compared to products generated through spontaneous fattening,[9] but these differences are not understood from a gastrophysical perspective. However, since the force-feeding practice is questionable regarding animal welfare,[10] it puts forward the quest for finding alternative preparations that match the texture quality of foie gras.

Several studies have targeted liver pâté[11–13] and meat emulsion[14–16] texture and stability by varying either the lipid composition, introducing dietary fibers, or a combination of both. The main focus of these studies has been to obtain textural properties similar to the reference product, and simple attempts to quantify the microstructure and relating this to texture have been made.[11] So far, the mechanical properties of foie gras and liver pâté have not yet been compared, and the microstructure of neither has not been assessed in detail.

Optical microscopy has proven a valuable tool for unraveling the complex organization of biomaterials due to its nondestructive nature, high spatiotemporal resolution, and sectioning capabilities. While microscopy has been instrumental for understanding food structure, some issues remain regarding sample preparation, making imaging impractical or impossible, or even altering the native structures in the worst scenario. Further, although not being a methodological limitation, most food microscopy studies are applied qualitatively rather than quantitatively limiting their direct comparison and correlation to relevant parameters at different length scales, for example, mechanical properties.

In recent decades, coherent Anti-Stokes Raman scattering (CARS) microscopy and related techniques have emerged as powerful imaging techniques that have found increasing use in the biological and medical sciences. CARS microscopy requires minimal sample preparation without need for extrinsic staining and enables fast image acquisition (up to video rate, 30 fps) at high spatial resolution ($<1\,\mu$m) and deep inside tissue ($>100\,\mu$m). Contrast in the sample is based on intrinsic molecular vibrations targeted by simultaneous illumination of the sample with two lasers with an energy difference matching particular chemical bonds. By tuning the energy difference of the lasers, different molecular vibrations can be targeted, for example, the $-CH_2$ stretching mode of lipids at 2845 cm^{-1}, with signal produced being orders of magnitudes larger than spontaneous Raman scattering. In many respects, CARS is an ideal candidate for imaging food structures, yet so far, only very few applications are found.[16–18]

In this study, we assessed the textural differences between force-fed duck foie gras and spontaneously fattened duck liver pâté products. In light of their intrinsic high fat content, CARS microscopy and quantitative image analysis were used to determine microstructural parameters to explain the mechanical/textural differences between both types of liver products. Overall, we show that the correlation of mechanical properties and microstructures can provide valuable insight into the texture of complex multiphasic food materials.

II. MATERIALS AND METHODS

A. Meat emulsions preparation

Foie gras sample, FG1 (Domaine de Langlardie, Piegut Dordogne, France), is commercially available in French supermarkets and foie gras sample, FG2, was bought directly from the producer (La Ferme Schmitt, Bischoffsheim, France). The homemade pâté (HME) emulsions were prepared using 50% of spontaneously fattened duck liver (Leon Dupont, Notre Dame de Riez, France), 40% rendered duck fat (Bruno Siebert, Ergersheim, France), and 10% water and 2% NaCl (w/w) (AnalaR NORMAPUR, VWR Chemicals, Darmstadt, Germany). The comminution was performed with a Hallde vertical cutter blender VCB-62 (AB Hallde Maskiner, Kista, Sweden). A first chopping step of the liver was performed at 1500 rpm for 5 s, followed by a second step at 3000 rpm for 10 s. Sodium chloride was added to the liver and stirred shortly. Afterward, fat and water were added to the liver paste and emulsified following a two-step blending process: 1500 rpm for 15 s, followed by 3000 rpm for 30 s. Liquid nitrogen (50–100 ml) was added between each step for temperature control. The final batter had an average temperature of 15.3 ± 3.3°C ranging from 9.8 to 20.7°C. The batter was filled into plastic containers and cooked in a preheated oven at 80°C for 90 min. After heating, the samples were stored in a fridge at 5°C for cooling.

B. Rheological properties

Rheological measurements were performed with a Bohlin Instruments Gemini 200 rheometer (Malvern Panalytical Ltd., Malvern, UK) equipped with a 25-mm parallel plate geometry. To prevent sample slipping, both plates were covered with 80 grit sandpaper. Before placing under the geometry, the sample was shaped using a round stencil (ø25 mm) and sliced in thin disks. The gap size was stepwise adjusted to the thickness of the slices until an increase in the normal force was detected leading to gap sizes between 1100 and 1700 µm. Oscillatory amplitude sweeps were performed from 0.01% to 200% strain with a frequency of 1 Hz at 5°C, while recording the storage (elastic) modulus, G', and loss (viscous) modulus, G''. Each sample was at measured at least 3 times. The limit of the linear viscoelastic region (LVR) was determined as the strain at which a 10% deviation from the G'_0 was reached. The cross-point was determined as the strain where $G' = G''$.

C. Texture measurements

The hardness of foie gras and pâté samples was measured with a ZwickRoell Universal Testing Machine AllroundLine Z005 (ZwickRoell GmbH, Ulm, Germany).[19] Samples were trimmed into cylinders (ø25, 20 mm height). Penetration tests were performed using a steel rod probe (ø10 mm) with a speed of 1 mm/s, until a deformation of 75% of the sample height was reached. All measurements were performed at room temperature with samples cooled to 5°C. Each sample was measured at least three times. Sample hardness was calculated considering the maximum peak force during compression, while the initial slope of the compression curve was determined by linear regression of the first five points above a threshold from 0.01% strain, to estimate the elasticity of the samples.

D. Moisture analysis

The moisture content of the samples was measured with a Mettler-Toledo HS153 halogen moisture analyzer (Mettler-Toledo, Columbus, US). Around 0.5 g of each sample was spread onto a fiberglass filter paper and placed in the device. The drying temperature was set to 120°C with a time ramp of 3 min, and the switch-off criterion was 1 mg/180 s of weight change. Each sample was measured at least 3 times.

E. CARS microscopy

Coherent Anti-Stokes Raman scattering (CARS) microscopy characterization was performed using a Leica SP8 CARS microscope (Leica Microsystems GmbH, Mannheim, Germany) equipped with a picoEmerald (APE, Berlin, Germany) multi-photon laser as the light source. The Stokes beam was fixed at $\lambda = 1064.5$ nm, whereas the pump beam was tuned to $\lambda = 817$ nm to excite symmetric $-CH_2$ stretching (2845 cm^{-1}) for the visualization of fat in the samples. Epi-mode detection was performed using a non-descanned photomultiplier tube (PMT) detector. A filter cube was placed in the detection path with a laser-blocking short-pass filter at 750 nm, a dichroic mirror at 560 nm, and a broadband filter 650/210 BrightLine HC (AHF analysentechnik AG, Tübingen, Germany). All images were acquired with a 40× HC PL IRAPO 1.10 NA Leica objective at room temperature. The laser power was adjusted for each image to give a signal intensity of about 20% of the saturation limit. Foie gras and pâté samples were sliced and placed in an 8-well chamber with a #1.5 glass bottom (Ibidi GmbH, Gräfelfing, Germany) immediately before imaging. Images of size 1928 × 1928 $pixel^2$ with pixel size = 0.15 μm were recorded at 5 μm depth into the sample in seven different regions of interest per sample giving a total of 21 images as each of the different sample types (FG1, FG2, and HME) were measured in triplicate.

F. Image analysis

Images were processed with *Fiji* software.[20] First, an automatic threshold (Huang algorithm)[21] was applied to obtain binary images that allowed for the identification of individual fat particles. Particles below the resolution limit were considered as noise and excluded from further analysis, while clusters with boundaries not entirely included in the image frame were also excluded. The analysis of fat particles included the following parameters: mean particle number per image, particle area, total area occupied by particles as well as their perimeter, aspect ratio, circularity, and Feret's diameter. *Aspect ratio* (AR) is the ratio between the longest and shortest axis of an ellipsoid fitted in the particle area. By definition, AR = 1 is a perfect circle, while increasing values account for deviation from this shape. *Circularity* relates area and perimeter of the particle and accounts for the edge sharpness. It ranges between 0 and 1, where the maximum value corresponds to a smooth circle and decreasing circularity correlates with surface roughness. Feret's diameter is defined as the maximum distance between two points within the particle (also known as maximum caliper). For the characterization of large interconnected clusters, the size threshold was defined considering the 90th percentile (P90) of the cumulative frequency of particle size for each sample, which represents the 10% largest particles of the total population. The size threshold to compare the three P90 was calculated as the mean between maximum and minimum P90, which yielded a size threshold of 4500 μm^2.

G. Statistical analysis

All significant differences between pâté and each FG sample were calculated using *t*-test with a significance level of 5% ($\alpha = 0.05$) (Minitab 19, State College, PA, USA). Data for each meat emulsion were collected from a total of 21 images obtained from three independent samples (n = 3). To assess the correlation between microscopic features and rheological parameters, Pearson correlation coefficients were determined. The Pearson correlation coefficient is a measure of the degree of linear correlation between two data sets, calculated as the ratio between the co-variance of the two variables and the product of their standard deviations. This gives values between −1 and 1, and the extreme values correspond to perfect negative and positive linear correlation, while 0 corresponds to no linear correlation at all.

III. RESULTS

A. Rheological and textural assessment of foie gras and pâté emulsions

Mechanical properties of two commercial brands of foie gras *bloc*, FG1, and FG2, and a homemade duck liver pâté, HME, were studied through amplitude sweeps, in a rheometer determining the storage modulus, G', and loss modulus, G'', as a function of strain% (Fig. 1), and by compression deformation in a texture analyzer determining the force vs strain relation (Fig. 2). Main parameters from these analyses are summarized in Table I.

As seen from Fig. 1, in the linear viscoelastic region, LVR, for all three samples, $G' > G''$ meaning that the samples display more gel-like behavior than liquid behavior. As expected for gel structures, increasing strain results in a non-linear regime, where the structure yields, and G' decreases. Initially, samples still predominantly display gel-like properties, where also G'' decreases with increasing strain%, but after the cross-point $G'' > G'$, and the samples predominantly behave as fluids indicating complete fracture of the gel structure.

Clear differences in the mechanical response to shear strain can be seen between foie gras samples and the pâté sample. For FG1 and FG2, both G' and G'' are roughly an order of magnitude larger than that of the HME, with FG2 having a higher G' than FG1, denoting a stronger gel strength in these samples. While all three samples show a rather short range of viscoelastic deformation, HME displays a longer LVR and also a larger strain value at the cross-point reflecting a structure that is more resistant to fracture and flow. Moreover, HME is also less brittle than either of FG samples.

The large-scale compression-force deformation measurements support the previous results of the foie gras samples being stronger but

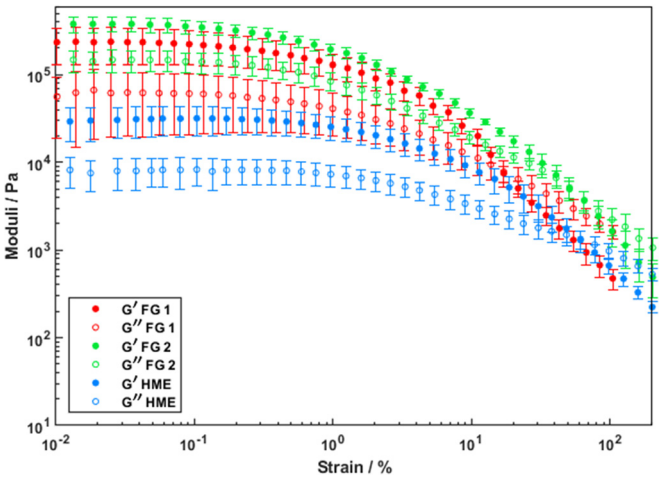

FIG. 1. Amplitude sweep measurements. Storage modulus G' (filled circles) and loss modulus G'' (open circles) are displayed for FG1 (red), FG2 (green), and HME (blue).

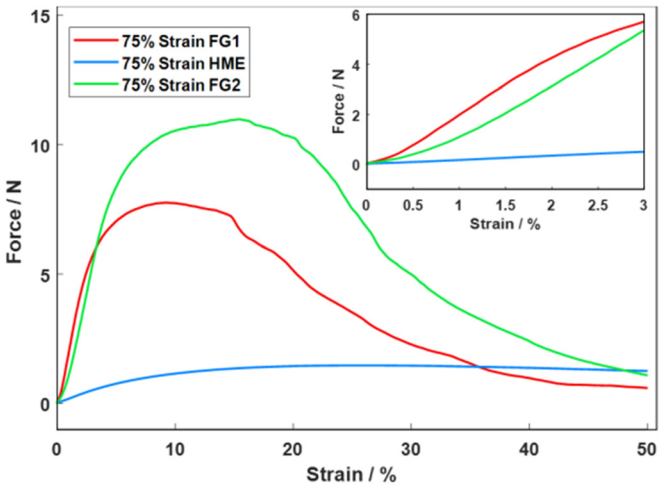

FIG. 2. Texture analysis. Compression curves for FG1 (red line), FG2 (green line), and HME (blue line). The inset shows a zoom-in of the initial part of the compression until 3% strain.

more prone to fracture. As seen from Fig. 2, the hardness (maximum peak force) of FG1 and FG2 is much larger than that of HME. For FG1 and FG2, after the peak is reached, the force rapidly decreases again showing structural breakdown of the sample, while for HME the force is kept at a constant, although lower, level. The initial slope of the deformation (see inset in Fig. 2) also confirms a much more elastic response to deformation in FG1 and FG2 as compared to HME.

B. Microscopic characterization

To get insight into the microstructures that underlie the observed differences in mechanical properties between foie gras and pâté, CARS microscopy was used to visualize the distribution of fat in the samples by probing the $-CH_2$ stretch (Fig. 3). A clear contrast between a particulate lipid phase (red) and a continuous water/protein phase (black) was observed for all samples. Qualitative inspection suggests that the overall area covered by lipid is similar between samples reflecting their compositional similarities. In all samples, the fat particles occur as clusters that are heterogeneously distributed within samples with varying size and morphological

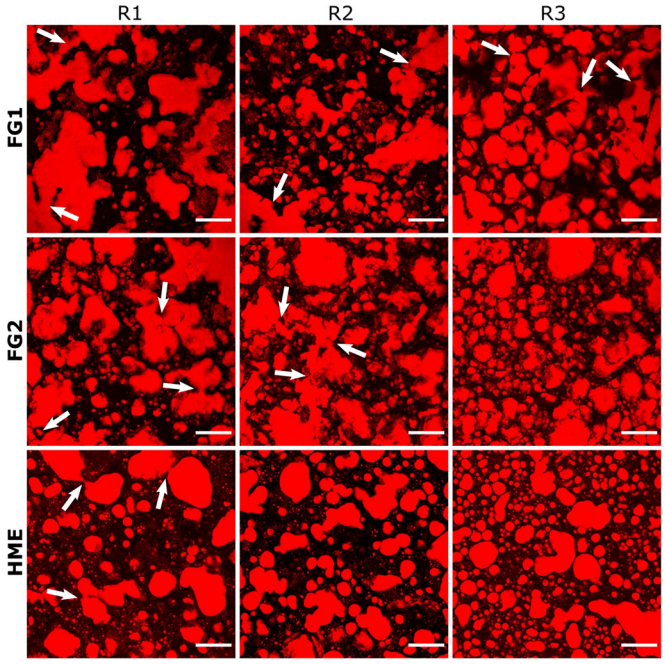

FIG. 3. CARS microscopy of fat distribution. Representative raw images of FG1 (first row), FG2 (second row), and HME (third row) from three replicates (columns R1, R2, and R3). White arrows indicate intra-cluster links. Image contrast was enhanced for the purpose of visually accentuating the lipid features. Scale bar = 50 μm.

features. Closer inspection of these fat particles suggests that the shape for FG1 and FG2 is more irregular than for HME, which has more round particles with smoother surfaces. It is further observed that fat particles are generally larger for FG1 and FG2 than HME, and that these large particles in many cases contain links between different parts of the particle as indicated with arrows in Fig. 3. These intra-cluster links are more frequently occurring in FG1 and FG2 samples as compared to HME.

In order to systematically compare the liver pâtés, we proceeded to quantify the number of fat particles along with the shape descriptors of each individual particle, that is, area, aspect ratio, circularity, perimeter, and Feret's diameter.

TABLE I. Physicochemical characterization of foie gras and pâté samples.

	Rheological parameters			Texture profile analysis		
Sample	G' (Pa)	LVR[a] (% strain)	Cross-point (% strain)	Hardness (N)[b]	Initial slope of compression curve[c]	Water content
HME	31 418 ± 8957	0.95 ± 0.22	56.05 ± 9.22	1.99 ± 0.46	0.24 ± 0.07	44.26 ± 0.85
FG1	199 010 ± 79 859	0.21 ± 0.09	30.44 ± 14.80	6.68 ± 0.87	0.64 ± 0.02	42.23 ± 0.29
FG2	357 801 ± 31 528	0.19 ± 0.005	45.24 ± 14.89	11.35 ± 0.18	0.35 ± 0.09	33.03 ± 1.63

[a]Linear viscoelastic region: region where applied stress is insufficient to cause structural breakdown (yielding), and hence, microstructural properties are being measured. This corresponds to the point at which G' becomes stress or strain dependent.
[b]Maximum peak force during compression.
[c]Fitted slope of the first data points.

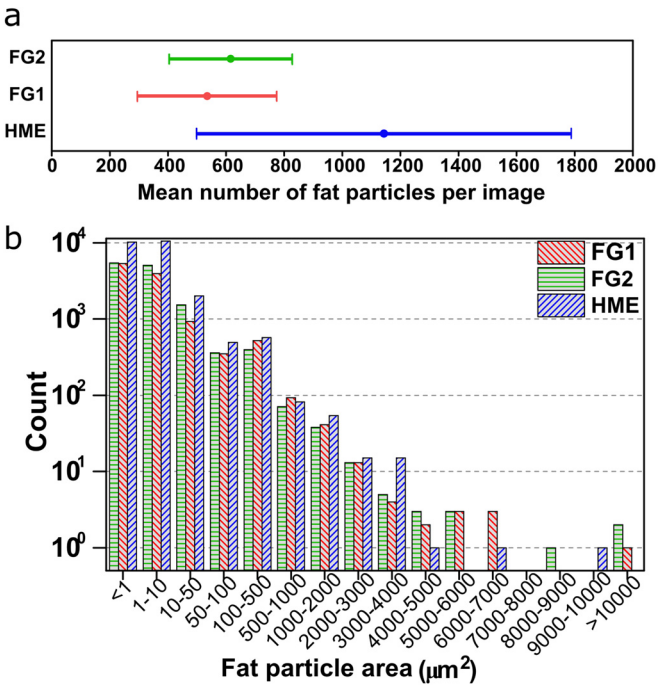

FIG. 4. Fat particle number and size. The mean number of fat particles (a) and fat particle size distribution (b) of FG1 (red), FG2 (green), and HME (blue).

C. Quantitative image analysis

The qualitative description of the microscopy images and fat particles in the foie gras and liver pâté was followed by quantitative image analysis to parameterize fat particle number and sizes (Fig. 4) and morphology (Fig. 5), as well as their correlation (Fig. 6). Image quantification further allows for directly relating microscopic features to the mechanical properties.

Quantification of the total area covered by fat confirms the overall compositional similarities between the samples, as it was FG1 = 43.3%, FG2 = 51.3%, and HME = 43.72%. As seen from the analysis of individual fat particles shown in Fig. 4, all samples have a large mean number of fat particles and a polydisperse size distribution in a range from approximately 1–10 000 μm^2 with about 50% of all particles being in the intermediate size range of 100–2000 μm^2 (corresponding to circular particles of ø6–30 μm). Clear differences are seen in the mean number of particles per image between FG samples (FG1 and FG2) and HME, with the latter having about twice as many particles as compared to FG1 and FG2 [Fig. 4(a)], which results in a significantly higher density of particles. The standard deviation of the mean particle number reflects differences between different regions of interest within each sample. This standard deviation was found to be significantly larger for HME as compared to FG1 and FG2, suggesting that the FG1 and FG2 samples are more self-similar in terms of particle distribution per unit area.

The size distribution of individual particles [Fig. 4(b)] reveals that the observed difference in total number of particles between FG1 and FG2 compared to HME mainly originates from the smallest size groups (<1 and 1–10 μm^2), where HME has considerably more particles that FG1 and FG2. Conversely, FG1 and FG2 samples both display higher counts of the larger fat clusters (>4000 μm^2) compared to HME. If the particle distributions are weighed by area (Fig. S1), these large particles account for ∼13% of the total area in both FG samples against 4% for pâté.

The mechanical properties of foie gras and pâté depend on the number of fat particles and the particle size distrubution and also on the morphology of the fat particles. As seen from Fig. 5, all samples have a wide distribution of aspect ratio and circularity, but clear differences are also seen between samples, and again, FG1 and FG2 show similar features to each other but differ from HME. In terms of roundness, the aspect ratio measures the shape elongation of the fat particles, and this is much closer to 1 (perfect circle) for HME than for FG1 and FG2 that both have aspect ratio distributions shifted toward higher values [Fig. 5(a)]. Circularity quantifies the surface roughness of the particles, and FG1 and FG2 samples share a left-skewed distribution of circularity toward 0 corresponding to fat particles markedly departing from the smooth surface of a perfect circle (circularity of 1) [Fig. 5(b)]. In contrast, HME has a centrosymmetric distribution of circularity, indicating that particles have a smoother surface, although not perfectly smooth.

Large fat particles can have a major impact on the textural properties of products such as foie gras and pâté. Based on the visual inspection of Fig. 3, interconnected clusters display a wide elongation

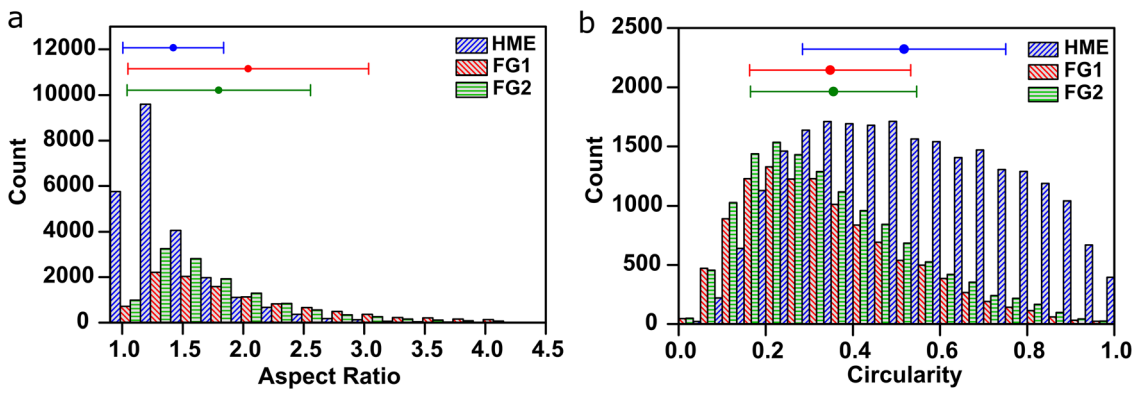

FIG. 5. (a) Aspect ratio distribution and (b) circularity distribution of HME (blue), FG1 (red), and FG2 (green).

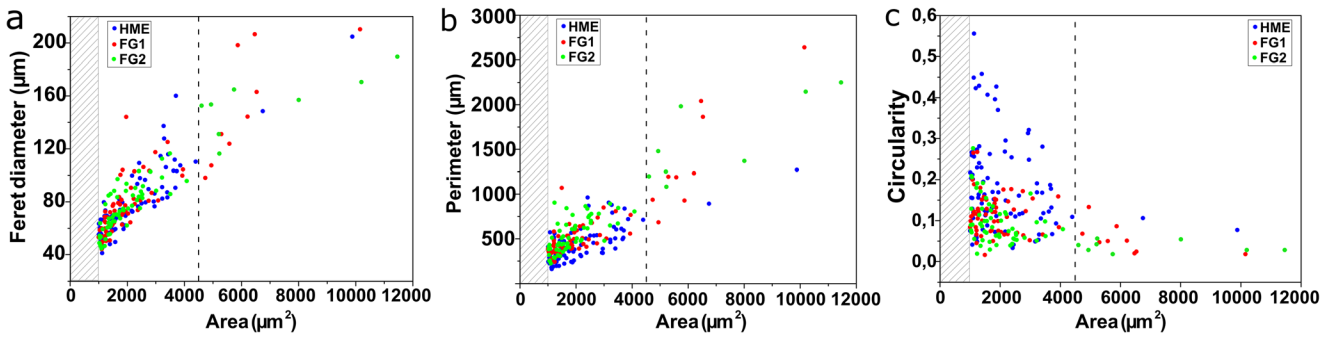

FIG. 6. Relationship between particle size (area) and (a) Feret's diameter, (b) particle perimeter, (c) circularity of HME (blue), FG1 (red), and FG2 (green). The dotted line represents the P90-based size threshold to quantify the largest clusters in each sample. For better visual understanding, only particles above 1000 μm^2 are plotted.

and irregular shapes, while covering large areas. Accordingly, Feret's diameter, perimeter, and circularity were calculated as main characterization variables for these connected clusters. The size threshold was set to 4500 μm^2, which corresponds to the on average 10% largest particles in all samples.

Plotting the Feret's diameter as a function of particle size [Fig. 6(a)] reveals a positive correlation, showing that the largest clusters in all samples are indeed the most elongated, which coincides with the observed interconnected clusters. Quantification of cluster number above 4500 μm^2 yielded higher counts in FG1 and FG2 samples than in HME. In turn, there is a higher contribution of these interconnected clusters to the total fat area in FG1 and FG2 than to HME: 12.7%, 11.3%, and 2.1%, respectively.

Positive correlation was also found between particle size and perimeter for all samples [Fig. 6(b)], but interestingly, when comparing clusters of similar size, FG1 and FG2 always have larger perimeter compared to HME, meaning that the large interconnected clusters in FG1 and FG2 have more irregular surfaces. This is well in line with the particle circularity being lower for FG1 and FG2 than for HME [Fig. 6(c)].

In summary and in agreement with the differences in mechanical properties, the quantitative image analysis also found considerable microstructural differences between foie gras samples and homemade pâté. The average fat particle in the homemade pâté is smaller, rounder, and smoother than in foie gras. Moreover, homemade pâté has more fat particles though this changes throughout the sample given its high spatial heterogeneity. Conversely, foie gras samples present a more homogeneous spatial distribution of relatively large interconnected fat particles with irregular surface and elongated shape.

D. Correlation between microscopic descriptors and textural parameters

To relate the microscopic distribution and morphology of fat particles to the mechanical properties of foie gras and pâté, correlation coefficients between measured microscopic descriptors and mechanical parameters were calculated. These data are summarized in Table II. As can be seen in the table, the initial storage modulus G'_0 and the sample hardness have strong positive correlations with Feret's diameter and particle perimeter, but a strong negative correlation with fat spatial heterogeneity and particle circularity. This suggests that increased gel strength is associated with the presence of large, elongated particles of irregular shape, which are distributed evenly throughout the sample.

The initial resistance to deformation as represented by the limit of the LVR correlates strongly and positively with the circularity, total interfacial perimeter, and spatial heterogeneity of fat particles while correlating strongly negative with Feret's diameter, aspect ratio, and perimeter, showing that generally matrices with more, rounder, and smaller particles are less prone to fracture.

The cross-point of the systems also correlates strongly and positively with the circularity and total interfacial perimeter, while having a strong and negative correlation with aspect ratio. This suggests that having more, round, and smooth particles renders the matrices more resistant to complete fracture and flow.

IV. DISCUSSION

The textural properties of different categories of fatty duck liver-based emulsions, that is, commercial foie gras and homemade pâté, were investigated using rheology and texture analysis and found to be similar within product category but differ between. In comparison with duck liver pâté, foie gras samples had a higher gel strength and were more brittle. In contrast, the pâté was comparatively weaker and showed a higher resistance to structural fracture. To uncover the microstructural characteristics that underlie these textural differences, the distribution and structures of the fat in such fatty liver-based products were for the first time visualized using CARS microscopy. Recent studies have targeted how the microstructure of pâté is affected by fat content and type.[11–13] These studies used standard light microscopy to image samples that were fixed, stained, and embedded in paraffin. In contrast to this, CARS microscopy did not require any staining, fixation, or embedding, but native samples could be imaged directly within the sample matrix to give highly specific signal from the fat and high signal-to-noise ratio. Previously, only a simple quantitative analysis of pâté microstructure has been presented[11] only reporting an average fat particle size. Based on the acquired CARS microscopy images, we were able to perform a thorough quantitative image analysis that take both particle abundance, size, and shape factors into account in order to better uncover a relation between texture and microstructure. This image analysis confirmed that also at the microscopic level, the foie gras samples showed similar characteristics, which differentiate them from those of the homemade pâté. While fat particles in foie gras samples were relatively large, irregular in shape, and linked

TABLE II. Pearson coefficients for the correlation between microscopic and rheological parameters.

	Microscopic descriptors					
Rheological parameters	Spatial heterogeneity[a]	Feret's diameter	Aspect ratio	Perimeter	Total interfacial surface[b]	Circularity
G'	−0.865	0.945	0.602	0.993	−0.575	−0.828
LVR	0.999	−0.972	−0.937	−0.902	0.925	1.00
Flow point	0.820	−0.695	−0.978	−0.528	0.984	0.857
Hardness	−0.895	0.964	0.652	0.998	−0.626	−0.862

[a]Defined as the standard deviation of mean particle number.
[b]Perimeter summation of all particles in each sample.

together to form an interconnected fat network, the homemade pâté was characterized by having more, smaller, and rounder fat particles that were not interconnected.

In foie gras, the fat distribution originates from the natural distribution of fat developed during force feeding. The fat is physiologically deposited in vacuoles inside hepatocytes producing a physical enlargement of these cells, which also result in an increased production of extracellular proteins, mainly different types of collagen.[22] During the preparation of foie gras, only very mild shear rates are required, and therefore, most of the fat remains intact within cells during the preparation, as has been shown for liver sausages prepared under higher shear.[23] Even during the final cooking of the foie gras during which a temperature of 65–70°C is reached, the fat mainly remains trapped within cells, although fat droplet fusion may occur but in the raw liver cells.[24] Depending on the rate of the subsequent cooling, the polymorphs of the crystalline parts of fats will re-arrange inside the fat particles and introduce deformations in the final fat particle shape. Such deformations are seen in the CARS images (Fig. 3). The temperature ramp of preparation also causes denaturation and cross-linking of some liver proteins in the continuous aqueous protein phase. In this way, free non-self-cross-linked cysteines from serum albumins and vitelin-1 form a weakly cross-linked gel around the fat clusters.

On the other hand, the preparation of the homemade pâté uses rendered fat and involves a high-shear cutting process, which is performed at low temperatures to prevent thermal denaturation of liver proteins and to maintain the fat in a solid state. Therefore, the structure of the pâté is a result of a highly non-equilibrium process. During the comminution and mixing process, the solid fat is dispersed in the liver water–protein phase, which simultaneously develops into a viscoelastic matrix as globular albumin-type proteins mechanically denature and undergo morphological changes that increase their surface activity. This blocky distribution of hydrophilic and lipophilic amino acids of albumins and other liver proteins ensures a stable emulsion during cooking. At this point, fat droplets with higher circularity are formed by minimizing the interfacial energy. During the cooling process after the heating (cooking) process, fat particles formed are more likely to retain the highly circular droplet shapes since the distribution of fatty acids is sufficiently broad.[5] This is in agreement with the homemade pâté showing smaller and circular emulsion-type fat droplets (Figs. 4 and 5), which do not seem to be able to form networks on larger scales (Fig. 3). The CARS micrographs suggest the presence of occasional larger fat particles, but there is no indication that these large particles are interconnected forming a network.

To connect the microscopic morphological differences between foie gras and pâté samples with the corresponding observed differences in mechanical response, Fig. 7 depicts segmented CARS images that highlight characteristic fat particles features (green and red colored). The rows in Fig. 7 show typical fat distributions of foie gras and pâté under imagined progressive shear deformation from left to right. Large clusters are shown in green color. Foie gras displays large connected clusters, which form an irregular fat network, whereas in pâté, the largest clusters remain embedded among small fat droplets. Consequently, the contribution of the fat to the mechanical properties is quite different,[25] given that connected fat networks transport

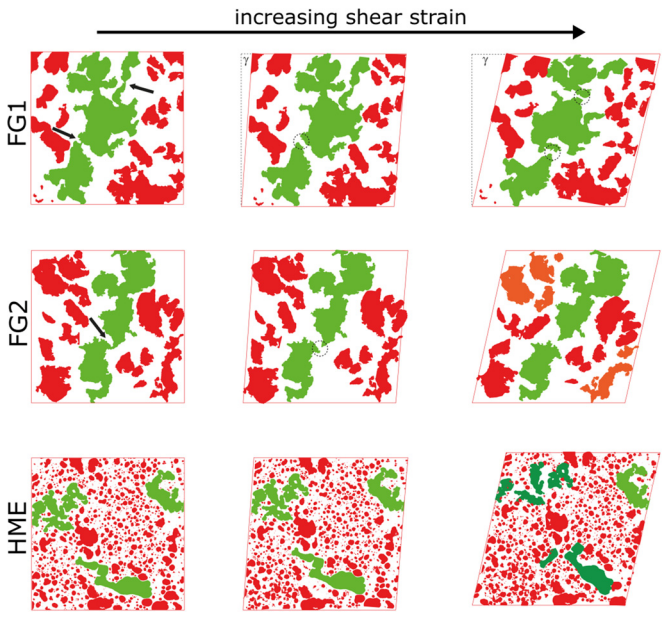

FIG. 7. The different pâtés show significantly distinct fat distributions. The fat droplets of HME are more spherical and well separated, whereas the foie gras show larger irregular shaped fat clusters, which form fat particle networks on larger scales. The arrows show the weak links in FG1 and FG2, which break at corresponding shear amplitudes, indicated by the circles. The fat cluster breaks further apart at higher shear rates (right). The separated dark green-colored larger clusters in HME break apart at corresponding shear rates and contribute mainly to a higher loss modulus G' at high shear deformations compared to FG1 and FG2.

mechanical forces/stresses and show characteristic changes of the storage G' and loss G'' moduli (Table I).[26,27]

The storage modulus contains mainly three contributions: (i) the weakly cross-linked protein matrix, (ii) the hydrodynamic part from the isolated fat particles acting as fillers,[28] and (iii) the contribution of the solid, crystalline fat network in the samples. The overall modulus remains constant under small shear deformations as long as the structure does not change, as it can be seen in Fig. 1 in the range between 10^{-2} and 10^{-1}% of strain. However, the connected clusters in foie gras show "weak links," which break subsequently under shear. The modulus decreases at deformations where the weak links in the largest clusters start to break apart. In addition, further softening by changing the matrix at moderate deformations imposed during the compression experiments is caused by disrupting hydrogen bonds[29] and electrostatic complexes between differently charged amino acids between neighboring protein sequences.[30]

The breaking of the fat network at the weak links defines the limit of the LVR range. From Figs. 3 and 7, it can be crudely estimated that, for example, the size of the largest cluster in FG2 is about 250 μm (Feret's diameter), whereas the distance between weak links can be estimated from Fig. 3 to be about 50 μm, suggesting a local shear deformation about 0.2% for breaking the weak links toward the end of the linear viscoelastic regime. Assuming a fine deformation processes before the break down of the particle network, this estimate agrees with the measured values.

The situation in the pâté is quite different. The contribution from the solid fat network to the storage modulus is missing, thus remaining mainly assigned to the weakly cross-linked protein network and the hydrodynamic reinforcement by the crystalline fat particles.[28] Not surprisingly, the hardness is lower, the storage modulus is lower, and the LVR is longer, as it is summarized in Table I.

These ideas are underlined by the results from the compression measurements shown in Fig. 2. The compression force increases steeply for foie gras samples and shows a maximum force indicating the fracture of the matrix. These observations are in accordance with results from rheology. At small compression deformations (<4%), the solid fat network resists the compression force until it breaks at the weak links. When the large fat clusters are broken, the deformations enter the plastic regime at strains larger than 40%. For pâté, the initial compression force is an order of magnitude lower, and this sample does not show a maximum force during compression, but instead the force linearly rises up to strains ~3%, as can be seen in the inset of Fig. 2, before entering the plastic regime, starting at strains larger than 20%. The compression force is transmitted mainly by the protein matrix, whereas the fat droplets contribute to a simple hydrodynamic reinforcement. The extended linear increment of the force for HME in the compression experiments corresponds thus to the extended LVR in the oscillatory amplitude sweep shown in Table I. Additionally, the distinguished initial force increments during compression (see inset of Fig. 2) reflect the overall difference in structure between foie gras and pâté. The foie gras shows a slight strain hardening and an inflection point and supports the contribution of a large-scale fat network in the solid emulsion. Differences in the mechanical behavior of the FG samples can be explained by the differences in fat content and distribution as well as water content, as has also been observed for pâté samples.[11] With less water content (Table I), higher total fat area, and interconnected fat clusters, FG2 has a stronger fat network and stronger gel structure. This leads to an increase in G'_0 and the hardness. In opposition to both FG samples, HME does not have the fat network structuring component although a similar content of water and fat as FG1.

The correlation parameters presented in Table II provide a neat summary of the relationship between fat microstructure and mechanical properties of fatty liver-based emulsions. This analysis suggests that having smaller, rounder, and smoother fat particles renders a softer gel-like emulsion, whereas the homogeneous distribution of larger, interconnected fat clusters provides a stronger structure.

V. CONCLUSIONS

Here, a comparative study on the texture and microstructure of fatty liver-based emulsions products was performed between two commercial brands of foie gras *bloc* and a homemade duck liver pâté. In terms of textural properties, the pâté prepared using spontaneously fattened duck liver and rendered fat yielded a much softer texture compared to both commercial foie gras *bloc* products. This was evidenced by a significantly smaller hardness and initial storage modulus G'_0 of the pâté compared to the foie gras samples.

CARS microscopy was used as a robust, label-free tool to characterize fat distribution in these fatty liver-based emulsions. Comparatively, the pâté lacked an interconnected network of large fat clusters present in foie gras samples. On the contrary, pâté had a higher concentration of small, round particles. These differences at the microscopic level between liver-based emulsions strongly correlated with mechanical differences. Stronger, more brittle gel correlated with larger, connected clusters with an irregular shape. Conversely, smaller and smoother particles correlated with a softer texture.

The microstructural characterization performed on fatty liver-based emulsions provided deeper insight into the causes of the textural differences observed. Furthermore, the correlation established between fat distribution and mechanical properties will allow for the improvement of pâté texture by tuning the microstructure to resemble that of foie gras. This can be achieved by adding, for example, industrially used food emulsifiers and/or liver-occurring proteins such as collagen, into the liver batter.

SUPPLEMENTARY MATERIAL

See the supplementary material for the fat particle size distribution weighed by area of the foie gras *bloc* samples and homemade pâté.

ACKNOWLEDGMENTS

The authors acknowledge the support from the Danish Molecular Biomedical Imaging Center (DaMBIC, University of Southern Denmark), where all imaging was performed. This work has been supported by the Villum Foundation (Denmark) through its Villum Young Investigator Programme (M.P. Clausen, Grant No. 00025414). M. Bächle was gratefully funded by VAN HEES GmBH, Walluf, Germany.

AUTHOR DECLARATIONS

Conflict of Interest

The authors have no conflicts to disclose.

Author Contributions

M.A.V. was involved in CARS imaging, image analysis, statistical analysis, and the manuscript draft; M.B. performed sample preparation, texture analysis, and rheology measurements; A.S. supervised, provided materials, and contributed to funding; T.A.V. was involved in the project idea, interpretation, model development, supervision, writing, and manuscript review; and M.P.C. was involved in the experimental design, interpretation, supervision, writing, and manuscript review.

DATA AVAILABILITY

The data that support the findings of this study are available from the corresponding authors upon reasonable request.

REFERENCES

[1]J. Chen and A. Rosenthal, "1-food texture and structure," in *Modifying Food Texture*, Woodhead Publishing Series in Food Science, Technology and Nutrition, edited by J. Chen and A. Rosenthal (Woodhead Publishing, 2015), pp. 3–24.

[2]E. Foegeding, C. Daubert, M. Drake, G. Essick, M. Trulsson, C. Vinyard, and F. Van de Velde, "A comprehensive approach to understanding textural properties of semi- and soft-solid foods," J. Texture Stud. **42**, 103–129 (2011).

[3]M. T. Pedersen, P. L. Hansen, and M. P. Clausen, "Gastronomy unravelled by physics: Gastrophysics," Int. J. Food Des. **6**, 153–180 (2021).

[4]C. Bonnefont, C. Molette, F. Lavigne, H. Manse, C. Bravo, B. Lo, H. Rémignon, J. Arroyo, and M. Bouillier-Oudot, "Evolution of liver fattening and foie gras technological yield during the overfeeding period in mule duck," Poultry Sci. **98**, 5724–5733 (2019).

[5]F. S. Carrillo, L. Saucier, and C. Ratti, "Thermal properties of duck fatty liver (foie gras) products," Int. J. Food Prop. **20**, 573–584 (2017).

[6]R. Mandigo and O. Esquivel, "Emulsions and batters," in *Encyclopedia of Meat Sciences, Vol. 1: Chemistry and Physics of Comminuted Products* (Elsevier, 2014), pp. 283–288.

[7]I. Allais, "Emulsification," in *Handbook of Meat Processing* (John Wiley & Sons, Ltd, 2010), Chap. 7, pp. 143–168.

[8]M. Wu, Y. L. Xiong, J. Chen, X. Tang, and G. Zhou, "Rheological and microstructural properties of porcine myofibrillar protein–lipid emulsion composite gels," J. Food Sci. **74**, E207–E217 (2009).

[9]X. Fernandez, V. Lazzarotto, M.-D. Bernadet, and H. Manse, "Comparison of the composition and sensory characteristics of goose fatty liver obtained by overfeeding and spontaneous fattening1," Poultry Sci. **98**, 6149–6160 (2019).

[10]I. Rochlitz and D. Broom, "The welfare of ducks during foie gras production," Animal Welfare **26**, 135–149 (2017).

[11]B. E. Tiensa, S. Barbut, and A. G. Marangoni, "Influence of fat structure on the mechanical properties of commercial pate products," Food Res. Int. **100**, 558–565 (2017).

[12]S. Barbut, A. G. Marangoni, U. Thode, and B. E. Tiensa, "Using canola oil organogels as fat replacement in liver pâté," J. Food Sci. **84**, 2646–2651 (2019).

[13]S. Barbut, B. E. Tiensa, and A. G. Marangoni, "Partial fat replacement in liver pâté using canola oil organogel," LWT **139**, 110428 (2021).

[14]M. Youssef and S. Barbut, "Effects of protein level and fat/oil on emulsion stability, texture, microstructure and color of meat batters," Meat Sci. **82**, 228–233 (2009).

[15]M. Youssef and S. Barbut, "Physicochemical effects of the lipid phase and protein level on meat emulsion stability, texture, and microstructure," J. Food Sci. **75**, S108–S114 (2010).

[16]M. Han, M. P. Clausen, M. Christensen, E. Vossen, T. Van Hecke, and H. C. Bertram, "Enhancing the health potential of processed meat: The effect of chitosan or carboxymethyl cellulose enrichment on inherent microstructure, water mobility and oxidation in a meat-based food matrix," Food Funct. **9**, 4017–4027 (2018).

[17]M. Roeffaers, X. Zhang, C. Freudiger, B. Saar, X. Xie, M. van Ruijven, G. van Dalen, and C. Xiao, "Label-free imaging of biomolecules in food products using stimulated Raman microscopy," J. Biomed. Opt. **16**, 021118 (2011).

[18]T. Meyer, D. Akimov, N. Tarcea, S. Chatzipapadopoulos, G. Muschiolik, J. Kobow, M. Schmitt, and J. Popp, "Three-dimensional molecular mapping of a multiple emulsion by means of cars microscopy," J. Phys. Chem. **112**, 1420–1426 (2008).

[19]A. Terrasa, M. D. Staffolo, and M. Tomás, "Nutritional improvement and physicochemical evaluation of liver pâté formulations," LWT-Food Sci. Technol. **66**, 678–684 (2016).

[20]J. E. Schindelin, I. Arganda-Carreras, E. Frise, V. Kaynig, M. Longair, T. Pietzsch, S. Preibisch, C. T. Rueden, S. Saalfeld, B. Schmid, J.-Y. Tinevez, D. J. White, V. Hartenstein, K. W. Eliceiri, P. Tomançak, and A. Cardona, "Fiji: An open-source platform for biological-image analysis," Nat. Methods **9**, 676–682 (2012).

[21]L.-K. Huang and M.-J. J. Wang, "Image thresholding by minimizing the measures of fuzziness," Pattern Recognit. **28**, 41–51 (1995).

[22]B. Lo, N. Marty-Gasset, C. Pichereaux, C. Bravo, H. Manse, R. Domitile, and H. Rémignon, "Proteomic analysis of two weight classes of mule duck 'foie gras' at the end of an overfeeding period," Front. Physiol. **11**, 569329 (2020).

[23]L. Steen, I. Fraeye, O. Goemaere, L. Sifre, B. Goderis, H. Paelinck, and I. Foubert, "Effect of salt and liver/fat ratio on microstructure, emulsion stability, texture and sensory mouth feel of liver paste," Food Bioprocess Technol. **7**, 2855–2864 (2014).

[24]L. Théron, T. Astruc, M. Bouillier-Oudot, C. Molette, A. Vénien, F. Peyrin, Z. Vitezica, and X. Fernandez, "The fusion of lipid droplets is involved in fat loss during cooking of duck 'foie gras,'" Meat Sci. **89**, 377–383 (2011).

[25]T. A. Vilgis, G. Heinrich, and M. Klüppel, *Reinforcement of Polymer Nano-Composites: Theory, Experiments and Applications* (Cambridge University Press, 2009).

[26]G. Huber, T. A. Vilgis, and G. Heinrich, "Universal properties in the dynamical deformation of filled rubbers," J. Phys.: Condens. Matter **8**, L409 (1996).

[27]B. Joshi, S. Beccard, and T. A. Vilgis, "Fractals in crystallizing food systems," Curr. Opin. Food Sci. **21**, 39–45 (2018).

[28]G. Huber and T. A. Vilgis, "On the mechanism of hydrodynamic reinforcement in elastic composites," Macromolecules **35**, 9204–9210 (2002).

[29]C. G. Cummings and A. D. Hamilton, "Disrupting protein–protein interactions with non-peptidic, small molecule α-helix mimetics," Curr. Opin. Chem. Biol. **14**, 341–346 (2010).

[30]S. Kumar and R. Nussinov, "Close-range electrostatic interactions in proteins," ChemBioChem **3**, 604–617 (2002).